VERIZONA PUBLISHER
Publishing Your Ideas

www.verizonaonlinepublishing.com
Vol: 1, Issue: 1

Journal of Nanoscience with Advanced Technology

Hydrogen storage in Lithium, Sodium, and Potassium nanoparticles

M. M. Sigalas

Department of Materials Science, University of Patras, 26504 Patras, Greece

***Corresponding author:** MM Sigalas, Department of Materials Science, University of Patras, 26504 Patras, Greece; Email: *sigalas@upatras.gr*

Article Type: Research, **Submission Date**: 1 May 2015, **Accepted Date:** 12 May 2015, **Published Date:** 8 June 2015.

Citation: M. M. Sigalas (2015) Hydrogen storage in Lithium, Sodium, and Potassium nanoparticles. J Nanosci Adv Tech 1(1): 12-16. doi: https://doi.org/10.24218/jnat.2015.03.

Abstract

Using Density Functional Theory (DFT), the desorption energies of Hydrogen in Lithium, Sodium, and Potassium nanoparticles is calculated. The type of nanoparticles studied were M_nH_{xn} with M=Li, Na, K and n varying from 2 up to 30. For each nanoparticle, several different geometries were studied in order to find the one with the lowest energy. The results were compared with similar calculated results for Beryllium and Magnesium nanoparticles. Mixed $Li_{n-x}Na_xH_n$ nanoparticles were also studied.

Introduction

Hydrogen is widely considered as a fuel of the future because it is environmentally friendly and it has high gravimetric (MJ/Kg) energy density (almost three times higher than hydrocarbons [1]). However, the major problem that needs to overcome is its storage. For practical applications, hydrogen needs to be stored in small volumes using materials that are light weight. These are difficult requirements since hydrogen in normal temperatures and pressures is a gas and even in its liquid form, it has about three time smaller volumetric energy density (MJ/m^3) than hydrocarbons [1]. Metal hydrides are promising materials for hydrogen storage with attractive gravimetric (wt% H) and volumetric ($Kg\,H\,m^{-3}$) densities [2]. More recently, nanostructured metal hydrides have attracted a lot of interest [3-5]. They have several order of magnitude surface to volume ratio relative to their bulk counterparts and their reaction kinetics and hydrogen diffusion are expected to improve [3-5].

Here, the desorption energies of nanostructured Li, Na, and K hydrides are studied using density functional theory (DFT). LiH has the highest hydrogen content than any hydride. However, it reacts explosively with water, there are several stability issues with LiH and it requires high temperatures for H removal [2]. For those reasons, LiH is not actually used in any practical applications. On the other hand, Li is used in several other compound hydrides (e.g. $LiAlH_4$ and $LiBH_4$ [2,6]). Also, carbon nanotubes, C_{60} and graphene doped with Li show significantly increased H content [7]. Similarly, Na is also used in compound hydrides ($NaAlH_4$) with improved kinetics and low temperature release of hydrogen [8]. So, even though it is our future goal to study compound hydrides containing Li and/or Na, it would really helpful to know desorption energies and the characteristics of simple LiH and NaH nanoparticles. Another motivation of the present study is to compare with similar calculations of Be_nH_m [9] and Mg_nH_m [10] nanoparticles. As for the KH nanoparticles, even though it does not have any practical applications due to its low hydrogen content and high weight (of K), and given (as will become clear from our calculations) the changes of the desorption energy from LiH to NaH nanoparticles, it is interesting to know how the desorption energy changes along the first column of the periodic table.

There are several experimental [11-13] and computational [14,15] studies of bulk LiH and NaH structures. But, there is much less published work on nanostructured LiH and NaH hydrides and all of them computational studies [16,17]. In the first study, small clusters with up to 4 Li or Na were considered [16], while in the second study the LiH molecule and $(LiH)_{2,3,4}$ clusters were identified by infrared spectra and they compared them with vibrational frequency calculation using the density functional method (DFT) [17]. There are also several computational studies of small Li and Na clusters [18,19].

Computational Techniques

The same procedure is followed as in previous computational studies of Be_nH_m [9] and Mg_nH_m [10] nanoparticles. The procedure is briefly described below.

For each nanoparticle M_n or M_nH_m (M=Li or Na or K), at least 10 different initial geometries were tested and fully optimized with the PBE functional [20]. The one with the lowest energy is used for the calculation of the desorption energy with the formula:

Before, the calculation of the desorption energy, the binding energy of selected small size nanoparticles was calculated with seven different generalized-gradient approximation (GGA), hybrid GGA, and hybrid meta-GGA functionals (PBE [20], BP86 [21,22], PW91 [23], B97D [24], TPSSh [25,26], B3LYP [27,28], M06 [29]). For those small size nanoparticles, the geometry optimization was also performed with coupled-cluster theory, including single and double excitations (CCSD) [30,31]. For all the cases at their optimized geometries, single-point energy calculations were performed using the higher level method, CCSD(T), which includes triplet excitations non iteratively [30,31]. All the calculations were performed with the GAUSSIAN program package [32].

For example, in Table I, the binding energies (De) for Li_4, Li_4H_4, Li_6, and Li_6H_2 are shown calculated with different functionals. The first line in each nanoparticle shows the De calculated after

geometry optimization with the particular functional. The second line in each nanoparticle shows the De calculated at a single point energy with CCSD(T). For Li_4, the De of the second line is 2.9 eV for all the functionals (except for B97D which is slightly smaller, 2.88 eV) and it is the same as the much more accurate (and extremely time and memory consuming) CCSD(T) calculation. This is a clear indication that all the functionals give the same optimized geometry as the much more accurate CCSD(T) calculation. This conclusion holds for all the nanoparticles shown in Table II and it is the same for nanostructured magnesium [10] and beryllium [9] hydrides.

It is also the same conclusion for similar nanostructured sodium and sodium hydride (Na_4, Na_4H_4, Na_6, and Na_6H_2) shown in Table II. However, comparing the De of the first line (the binding energies for each functional) with the De of CCSD(T) calculation (last column), there are significant differences reaching a value of up to 30%. In particular for all the Li and LiH nanoparticles shown in Table I, the De results obtained with M06 functional have less than 2% difference with the ones obtained with CCSD(T). Other functionals such as B3LYP and TPSSh performed almost equally well with maximum differences from the CCSD(T) results reaching a value of about 11%. For the Na and NaH nanoparticles shown in Table II, the differences between the De results calculated with M06 and the CCSD(T) results are higher (especially for the Na nanoparticles) reaching a maximum value of 18%. Other functional such as B3LYP, TPSSh, PW91, and BP86 gave slightly smaller differences. However, for consistency and for being able to compare the Li and Na results, the M06 functional is chosen for all the energy calculations. For the geometry optimization, the PBE functional is used which needs less memory and it is faster. In all the cases the zero point vibrational energies (ZPE) were also calculated.

Li and LiH nanoparticles

Figure 1 shows the lowest energy structures for the Li_8H_m nanoparticles. The lowest energy structure of the Li_8 has an almost perfect Cs symmetry and it is the same as the one reported in Refs 18 and 19. The lowest energy structures of Li_8H_2, Li_8H_4, Li_8H_6, and Li_8H_8 have an almost C2v, D2d, C2, and S4 symmetries. In these cases and in general in all the Li_nH_m nanoparticles, hydrogen atoms tend to be located in the surface of the nanoparticles between three lithium atoms. Also for all the Li_nH_m nanoparticles, they are able to hold m=n number of hydrogen atoms. Adding more H, a hydrogen molecule is formed away from the nanoparticles. This is clearly seen in Figure 1 for the case of Li_8H_{10} which is actually formed from the Li_8H_8 structure with a hydrogen molecule slightly away from its surface.

The desorption energies for Li_nH_m nanoparticles and n=6, 8, 10, 15, 20, and 30 are shown in Figure 2.

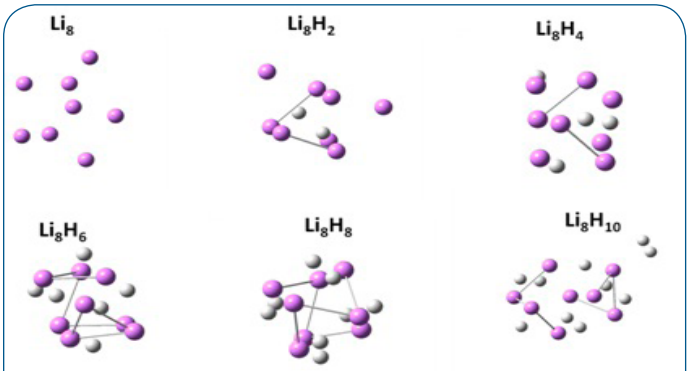

Figure 1: The optimized geometries for the Li8Hm nanoparticles

Table I: Binding Energies (De) in eV

structure	property	PBE	BP86	PW91	B97D	TPSSh	B3LYP	M06	CCSD(T)
Li_4	De/cc-PVTZ	2.65	2.60	2.75	3.30	2.83	2.54	2.94	
	De/CCSD(T)	2.90	2.90	2.90	2.88	2.90	2.90	2.90	2.90
Li_4H_4	De/cc-pVTZ	15.21	15.82	15.45	17.15	16.27	16.08	16.05	
	De/CCSD(T)	15.76	15.76	15.76	15.67	15.76	15.76	15.76	15.76
Li_6	De/cc-pVTZ	5.06	4.83	5.18	5.89	5.21	4.61	5.31	
	De/CCSD(T)	5.20	5.19	5.20	5.12	5.20	5.18	5.20	5.20
Li_6H_2	De/cc-pVTZ	11.45	11.55	11.66	13.19	12.10	11.50	12.00	
	De/CCSD(T)	11.76	11.77	11.76	11.76	11.76	11.76	11.77	11.77

Table II: Binding Energies (De) in eV

structure	property	PBE	BP86	PW91	B97D	TPSSh	B3LYP	M06	CCSD(T)
Na_4	De/cc-PVTZ	1.90	1.72	1.97	3.28	1.99	1.64	2.19	
	De/CCSD(T)	1.84	1.84	1.84	1.79	1.85	1.83	1.85	1.85
Na_4H_4	De/cc-pVTZ	11.89	12.47	12.4	14.56	12.99	12.49	13.30	
	De/CCSD(T)	12.52	12.52	12.52	12.49	12.52	12.52	12.50	12.53
Na_6	De/cc-pVTZ	3.58	3.22	3.68	5.54	3.65	3.03	3.91	
	De/CCSD(T)	3.32	3.33	3.32	3.26	3.34	3.31	3.33	3.35
Na_6H_2	De/cc-pVTZ	8.53	8.52	8.72	11.38	9.18	8.35	9.59	
	De/CCSD(T)	8.71	8.73	8.72	8.64	8.74	8.71	8.75	8.75

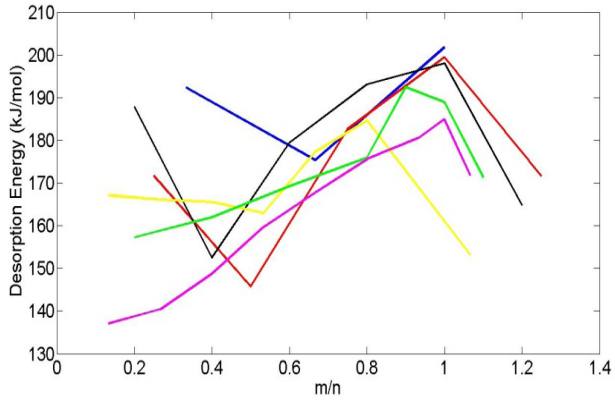

Figure 2: The desorption energy (without the ZPE) for Li_nH_m nanoparticles for **n=6, 8, 10, 15, 20, and 30** (blue, red, black, yellow, green, and magenta lines, respectively)

Ignoring some high desorption values for the small n (6, 8, and 10) and m=2 cases, the general trend is an almost constant increase of desorption energy as the number of hydrogen atoms (m) increases until it reaches the value of n (the nanoparticle has equal number of Li and H atoms in that case). After that, there is drop of the desorption energy since, as it was mentioned earlier, the nanoparticles cannot hold any additional hydrogens, instead, hydrogen molecules are formed away from the surface of the nanoparticles. This behavior is similar with the one found in Mg_nH_m nanoparticles [10] although magnesium hydride nanoparticles can hold up to m=2n hydrogen atoms. The same picture is obtained when the ZPE is added in the calculation of desorption energy (Figure 3) but now the energies are 5-15 kJ/mol smaller than the corresponding values without the ZPE.

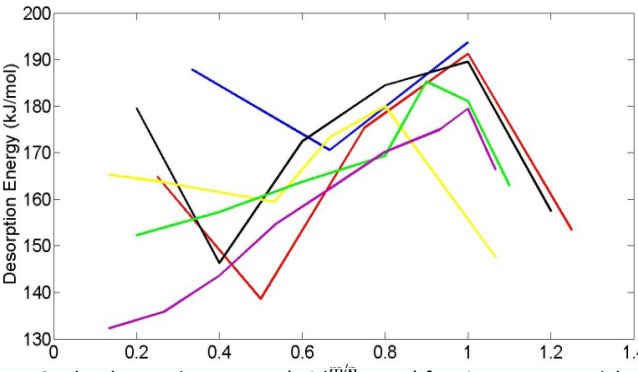

Figure 3: The desorption energy (with the ZPE) for Li_nH_m nanoparticles for **n=6, 8, 10, 15, 20, and 30** (blue, red, black, yellow, green, and magenta lines, respectively)

Figure 4 shows the desorption energy for the Li_nH_n (fully hydrogenated) nanoparticles. Ignoring the n=4 case, there is a drop of desorption energy as n increases. This drop becomes smaller (saturates) for higher values of n (20 and 30). The curves for desorption energies with and without ZPE follow the same trend with the energies with ZPE being 5-10 kJ/mol smaller. From the ZPE curve (blue line in Figure 4), one can see that the desorption energy seems to saturates at around 175-180 kJ/mol for high values of n. There are experimental data only for the bulk LiH. The experimental values are 178.56 kJ/mol [11], 180 kJ/mol [13], and 232.6 kJ/mol [12] (note that all the desorption energies reported here are in kJ/mol H_2). The present desorption energies of Li_nH_n with high values of n are in a very good agreement with at least two of the experimental results for the bulk LiH. There are also in good agreement with calculated results for the bulk LiH which are 173.7 kJ/mol [14], and 169.8 kJ/mol [15]. The present results for the desorption energy of large Li_nH_n nanoparticles, are more than two times higher than the corresponding calculated energies for Mg_nH_{2n} nanoparticles (about 54 kJ/mol for the amorphous and 76.5 kJ/mol for the crystalline for high values of n) [10], and almost ten times higher than the Be_nH_{2n} nanoparticles (about 18.9 kJ/mol for high values of n) [9].

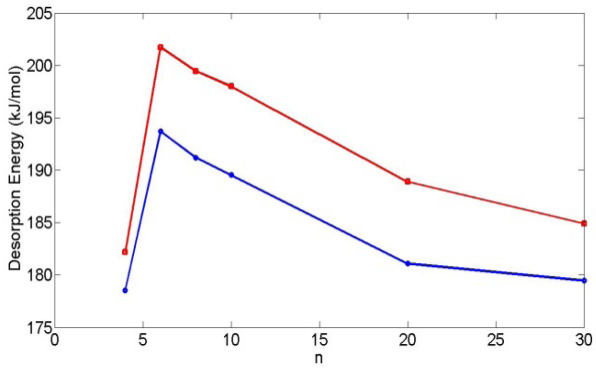

Figure 4: The desorption energy with and without (blue and red lines, respectively) the ZPE for Li_nH_n nanoparticles

Na and NaH nanoparticles

The lowest energy structures for the Na and NaH nanoparticles have similar geometries as the corresponding Li and LiH nanoparticles but they are slightly bigger in size. For example, the $Na_{30}H_{30}$ has an average diameter of 0.9 nm while $Li_{30}H_{30}$ has an average diameter of 0.8 nm. Desorption energy also has the same trend as in LiH nanoparticles when the hydrogen content increases. Figure 5 shows the desorption energy for Na_nH_m nanoparticles as the hydrogen content (m) increases. Desorption energy increases as m increases in almost all the cases with only exception the Na_6H_4 and $Na_{10}H_4$. The maximum number of hydrogen atoms is reached when m=n and after that, additional hydrogen atoms form a hydrogen molecule away from the nanoparticle.

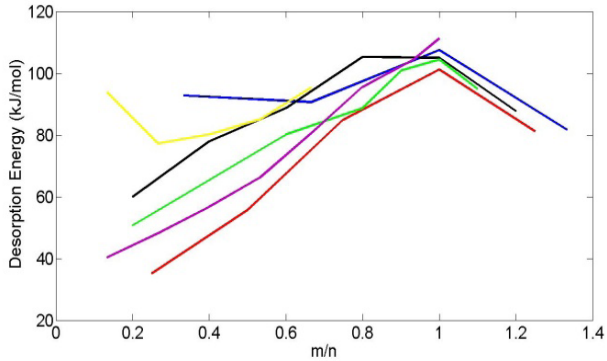

Figure 5: The desorption energy (with the ZPE) for Na_nH_m nanoparticles for **n=6, 8, 10, 15, 20, and 30** (blue, red, black, yellow, green, and magenta lines, respectively)

Desorption energy for the fully hydrogenated nanoparticles (m=n) is shown in Figure 6. The difference between the energy values with and without ZPE is less than 4 kJ/mol in all the cases. This is smaller than the same difference in Li_nH_n nanoparticles (see Figure 4). Besides some fluctuations for small n, desorption

energies for n=10, 20, and 30 have similar values between 105 and 111 kJ/mol. These agree well with experimental values for the heat of formation of bulk NaH (113.8 kJ/mol [11] and 113 kJ/mol [12]). They are about 45% lower than the corresponding desorption energies of Li_nH_n nanoparticles.

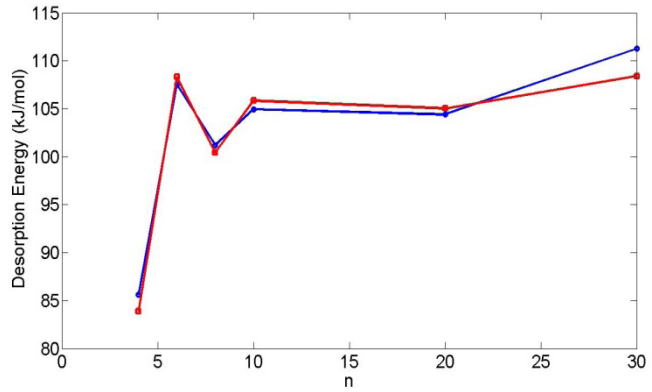

Figure 6: The desorption energy with and without (blue and red lines, respectively) the ZPE for Na_nH_n nanoparticles

$Li_{n-x}Na_x$ and $Li_{n-x}Na_xH_n$ nanoparticles

From the previous two sections it becomes clear that Li_nH_n nanoparticles, even though they are light weight, they have significantly high desorption energies making them unattractive for hydrogen storage. On the other hand, Na_nH_n nanoparticles have significantly lower desorption energies but they have significantly higher weight. It would be interesting to see how mixed $Li_{n-x}Na_xH_n$ nanoparticles would behave.

As a tested case, the $Li_{20}H_{20}$ was chosen and one Li atom was replaced with a Na atom. Several initial configurations were tested and fully optimized. The procedure was continued by replacing an additional Li atom until all Li atoms were replaced with Na atoms. The inverse procedure was also explored starting from $Na_{20}H_{20}$ and replacing Na atoms with Li atoms. For each $Li_{n-x}Na_xH_n$ nanoparticles, the lowest energy structure was chosen. Desorption energies for $Li_{n-x}Na_xH_n$ nanoparticles as a function of x are shown in Figure 7. Besides some small drops for x= 2 and 10, it follows almost a straight line. A linear fit of the desorption energies with ZPE gives 175.974 – 3.834 x. The $Li_{n-x}Na_xH_n$ nanoparticles with n=10 were also examined with similar results.

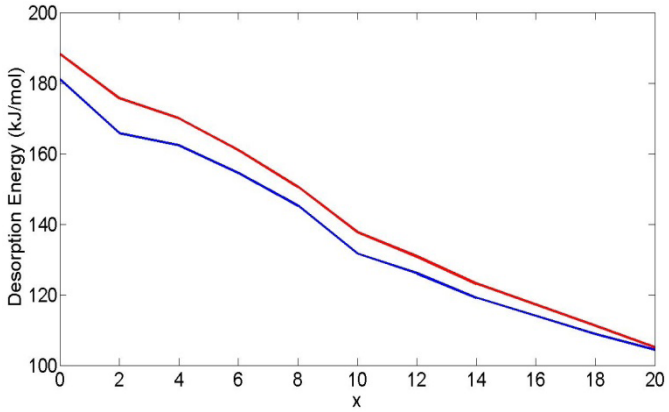

Figure 7: The desorption energy with and without (blue and red lines, respectively) the ZPE for $Li_{n-x}Na_xH_n$ nanoparticles and n=20

K and KH nanoparticles

As it was mentioned earlier, there is a significant drop of the Na_nH_m desorption energies relative to the Li_nH_m ones. The question then arises about the desorption energies of KH nanoparticles. For that reason, K_n and K_nH_m nanoparticles with n=10 and 20 were also studied. Figure 8 shows, their desorption energies as m increases. The behavior is similar as in LiH and NaH nanoparticles. Desorption energy increases as the hydrogen content (m) increases in each nanoparticle until it reaches the value of m=n. Beyond that value, the nanoparticles cannot absorb any more hydrogen; instead hydrogen molecules are formed close to the surface of the nanoparticles. For $K_{20}H_{20}$, desorption energy is about 89 kJ/mol. This is about 15% less than the value for $Na_{20}H_{20}$. Taking into account that the weigh is significantly increases in KH nanoparticles and the not so significantly lower desorption energy, KH nanoparticles could not find any potential applications in hydrogen storage.

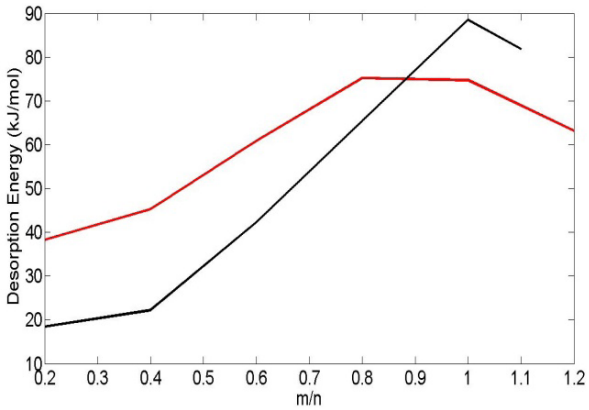

Figure 8: The desorption energy (with the ZPE) for K_nH_m nanoparticles for **n=10, 20** (red, black, lines, respectively)

Conclusions

A computational study of M_n and M_nH_m with M=Li, Na, K and n varying from 2 up to 30 was performed using Density Functional Theory (DFT). The calculated desorption energies for almost all the nanoparticles were increasing as the hydrogen content (m) increases until m=n. Beyond that m, no more hydrogen atoms can be absorbed and hydrogen molecules are formed away from surface of the nanoparticles. For high values of n (20 and 30), desorption energies of fully hydrogenated nanoparticles (m=n) saturate to about 175 kJ/mol and 110 kJ/mol for LiH and NaH nanoparticles. Desorption energy for $K_{20}H_{20}$ is 89 kJ/mol. $Li_{n-x}Na_xH_n$ nanoparticles were also studied with their desorption energies having an almost linear dependence on x.

Acknowledgements

I would like to thank Mr. G. Mallis for helping in some of the calculations, Dr. E. N. Koukaras and Prof. A. D. Zdetsis for helpful discussions. This work is partially supported from the SYNERGASIA2011 program.

References

1. Gupta RB, editor. Hydrogen fuel: Production, transport, and storage. Boca Raton: CRS Press; 2009.
2. Sakintuna B, Lamari Darkrim F, Hirscher M. Metal hydride materials for solid hydrogen storage: A review. Intern. J. Hydrogen Energy. 2007; 32(9):1121-1140. doi:10.1016/j.ijhydene.2006.11.022.
3. Wu H. Strategies for the improvement of the hydrogen storage properties of metal hydride materials. ChemPhysChem. 2008; 9(15):2157-62. doi: 10.1002/cphc.200800498.
4. Kelly MT. Perspective on the storage of hydrogen: Past and Future. Struct. Bonding. 2011; 141:169-201. doi: 10.1007/430_2011_46.
5. Fichtner M. Properties of nanoscale metal hydrides. Nanotechnology. 2009; 20(20):204009. doi: 10.1088/0957-4484/20/20/204009.
6. Ravnsbak DB, Jensen TR. Mechanism for reversible hydrogen storage in LiBH4-Al. J. Appl. Phys. 2012; 111:112621. doi: http://dx.doi.org/10.1063/1.4726244.
7. Dimitrakakis GK, Tylianakis E, Froudakis GE. Nano Lett; 8:3166–3170.
8. Jain IP, Jain P, Jain A. Novel hydrogen storage materials: a review of lightweight complex hydrides. J. Alloys Compounds. 2010; 503(2):303. doi:10.1016/j.jallcom.2010.04.250.
9. Zdetsis AD, Sigalas MM, Koukaras EN. *Ab initio* theoretical investigation of beryllium and beryllium hydride nanoparticles and nanocrystals with implications for the corresponding infinite systems. Phys. Chem. Chem. Phys. 2014; 16(27):14172. doi: 10.1039/c4cp01587h.
10. Koukaras EN, Zdetsis AD, igalas MM. *Ab Initio* Study of Magnesium and Magnesium Hydride Nanoclusters and Nanocrystals: Examining Optimal Structures and Compositions for efficient Hydrogen Storage. J Am Chem Soc. 2012; 134(38):15914-15922.
11. Messer CE, Fasolino LG, Thalmayer CE. The heat of formation of Lithium, Sodium, and Pottasium Hydrides. J. Am Chem. Soc. 1955; 77:4524. doi: 10.1021/ja01622a025.
12. Grochala W, Edwards PP. Thermal Decomposition of the Non-Interstitial Hydrides for the Storage and Production of Hydrogen. Chem Rev. 2004; 104(3):1283-316.
13. Luo W. (LiNH2-MgH2): A viable hydrogen storage system. J. Alloy Compounds. 2004; 381(1-2,3):284-287. doi:10.1016/j.jallcom.2004.03.119.
14. Wolverton C, Ozolins V, Asta M. Hydrogen in aluminum: First-principles calculations of structure and thermodynamics. Phys Rev B. 2004; 69:144109. doi: http://dx.doi.org/10.1103/PhysRevB.69.144109.
15. Napan R, Peltzer y Blanca EL. First principles studies of lithium hydride series for hydrogen storage. Intern. J. Hydrogen Energy. 2012; 37(7):5784-5789. doi:10.1016/j.ijhydene.2011.12.117.
16. Chen YL, Huang CH, Hu WP. Theoretical study on the small clusters of LiH, NaH, BeH_2, and MgH_2. J. Phys. Chem. A. 2005; 109(42):9627-36.
17. Wang X, Andrews L. Infrared spectra and theoretical calculations of lithium hydride clusters in solid hydrogen, neon and argon. J Phys Chem A. 2007; 111:6008-19.
18. Gardet G, Rogemond F, Chermette H. Density functional theory study of some structural and energetic properties of small lithium clusters. J. Chem. Phys. 1996; 105:9933.
19. Florez E, Fuentealba P. A theoretical study of alkali metal atomic clusters: from Li_n to Cs_n (n=2-8). Intern. J. Quant. Chem. 2009; 109(5):1080-1093. doi: 10.1002/qua.21906.
20. Perdew JP, Burke K, Ernzerhof M. Phys. Rev. Lett. 1996; 77:3865.
21. Becke AD. Phys. Rev. A. 1988; 38:3098.
22. Perdew JP. Phys. Rev. B. 1986; 33:8822.
23. Perdew JP, Burke K, Wang Y. Phys. Rev. B. 1996; 54:16533.
24. Grimme SJ. Comput. Chem. 2006; 27:1787−1799.
25. Tao JM, Perdew JP, Staroverov VN, Scuseria GE. Phys. Rev. Lett. 2003; 91:146401.
26. Staroverov VN, Scuseria GE, Tao J, Perdew JP. J. Chem. Phys. 2003; 119:12129.
27. Becke AD. J. Chem. Phys. 1993; 98:5648–5652.
28. Lee C, Yang W, Parr RG. Phys. Rev. B: Condens. Mater. Phys. 1988; 37:785–789.
29. Zhao Y, Truhlar DG. Theor. Chem. Acc. 2008; 120:215–241.
30. Purvis III GD, Bartlett RJ. A full coupled-cluster singles and doubles model - the inclusion of disconnected triples. J. Chem. Phys. 1982; 76:1910-18. doi: http://dx.doi.org/10.1063/1.443164.
31. Scuseria GE, Janssen CL, Schaefer III HF. An efficient reformulation of the closed-shell coupled cluster single and double excitation (CCSD) equations. J. Chem. Phys. 1988; 89: 7382-87. doi: http://dx.doi.org/10.1063/1.455269.
32. Frisch MJ, Trucks GW, Schlegel HB, Scuseria GE, Robb MA, Cheeseman JR, et al. Gaussian 09, Revision C.01, Gaussian Inc., Wallingford CT; 2009.